

# NA62: Ultra-Rare Kaon Decays

Phil Rubin  
George Mason University  
For the NA62 Collaboration

November 10, 2011

The primary goal of the experiment is to reconstruct more than 100  $K^+ \rightarrow \pi^+ \nu \bar{\nu}$  events, over two (machine) years of running, keeping systematic uncertainties at a level well below that of statistical uncertainties, so that the total uncertainty is of order 10%, about the level of theoretical uncertainties. Given a signal branching ratio of about  $8.5 \times 10^{-11}$ , and about a 10% detector acceptance, the detector needs to “see” roughly  $10^{13}$   $K^+$  decays. In order to keep background contamination below 10%, suppression must be at the  $10^{-12}$  level, within an uncertainty of less than 10%, so as not to inflate systematic uncertainties with the background subtraction.

Statistical sensitivity then requires a very high intensity kaon beam and optimized signal sensitivity. Systematic sensitivity will result from maximizing signal purity to reduce accidentals and minimizing material in the spectrometer to reduce multiple scattering. In addition, detector redundancies will permit internal cross-checking.

The signal,  $K^+ \rightarrow \pi^+ \nu \bar{\nu}$ , has a branching fraction of  $\mathcal{O}(10^{-10})$ . The primary backgrounds to this signal,  $K^+ \rightarrow \mu^+ \nu_\mu$  and  $K^+ \rightarrow \pi^+ \pi^0$ , have branching fractions of  $\mathcal{O}(1)$ , higher by ten orders of magnitude. These are two-body decays, while the signal is a three body decay, so kinematics, given outstanding resolution, can help distinguish them from signal. Unfortunately, even the best of systems suffers from non-Gaussian reconstruction tails. To make matters worse, the final states of these background are similar to that of the signal. The  $\pi^+$  is all that is detectable from the signal channel, as is the muon of the  $\mu^+ \nu_\mu$  background. Excellent particle identification can distinguish these even where kinematics might prove inadequate. The  $\pi^+ \pi^0$  final state has the same charged particle as the signal, but the  $\pi^0$  decays rapidly into two photons, two electrons and a photon, or four electrons. Should these secondary particles go undetected, and the kinematic measurements fall in the tails, the event may be mis-identified as signal. The detector thus needs to be hermetic. Several multi-body  $K^+$  decay channels, most not subject to kinematic differentiation from the signal channel, with branching fractions from  $\mathcal{O}(10^{-4})$  to  $\mathcal{O}(10^{-2})$ , are also backgrounds, which, to be rejected, must be detected and identified. These include radiative two-body decays as well as  $K^+ \rightarrow \pi^+ \pi^+ \pi^-$ ,  $K^+ \rightarrow \pi^+ \pi^0 \pi^0$ , and the semi-leptonic modes  $K_{e3}$  and  $K_{\mu 3}$ .

The experiment will be run in the north area extraction line of CERN’s SPS ring. It will use a relatively high-momentum  $K^+$  beam ( $75.00 \pm 0.75$  GeV/c), which can be delivered at high intensity, optimized for kaon flux relative to that of charged pions and protons ( $\approx 750$  MHz hadron beam,  $\approx 6\%$   $K^+$ , from  $1.1 \times 10^{12}$  protons/s during a spill). The decay-in-flight fixed-target technique will be employed, permitting the use of an extended detector array with redundant momentum and particle identification determinations.

The signature of the signal is a single, off-beam-axis, charged pion and nothing else. Backgrounds include not only essentially all other  $K^+$  decays, many listed above, but also accidental charged particles from secondary beam particle interactions and their decays. To manage this difficult experimental environment,

the NA62 detector [see Figure 1] has been designed for kinematic rejection, tight timing, hermetic vetoing, and redundant particle identification.

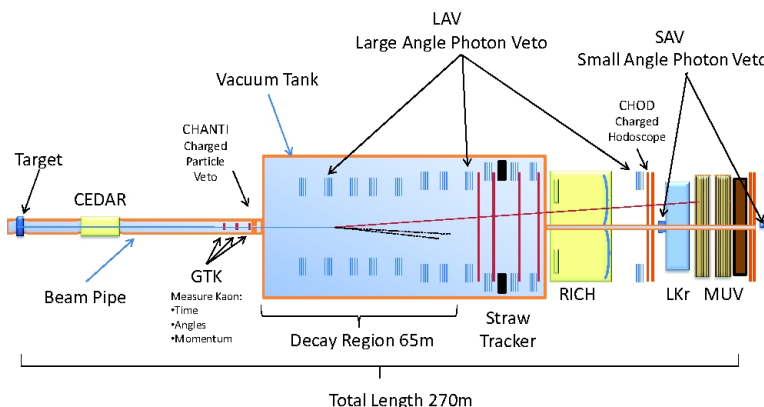


Figure 1: The NA62 Detector.

The NA62 detector will be in the beam line and experimental hall of the former NA48 experiment, whose liquid krypton electromagnetic calorimeter will be refitted with new power supplies and readout electronics and reused. A beamline differential Cerenkov detector, CEDAR, will be renovated with new optics and filled with hydrogen for charged-kaon identification. The NA48 hadron calorimeter will be refurbished for use as a muon detector, behind which a new scintillator array will serve as a fast muon veto. The NA48 charged-trigger hodoscope will either be renovated or replaced. Six additional new subdetector groups are being built: GIGATRACKER (GTK), CHANTI (charged particle veto), Large Angle Veto, Straw Tracker, RICH, and Small Angle and Beamline calorimeters.

Because characterizing the incoming kaon beam is essential for selecting events of interest and reducing backgrounds, the GTK is a pivotal component. It will provide precision measurements of this beam's momentum (relative uncertainty of 0.2%), time ( $\sim 150$  ps [rms]), and angle ( $\sim 16$   $\mu$ rad). See Figure 2 for test beam results with GTK proto-types. It is composed of three hybrid silicon pixel detector stations mounted around four achromatic magnets, and is in the beam line inside a vacuum tank, just before the primary elements of the NA62 detector. Pixel dimensions and station separations are optimized to deliver the required momentum and angular resolution. Angular resolution is also affected by the amount of material crossed by the beam at each station. A sensor thickness of 200  $\mu$ m, corresponding to 0.22% of a radiation length,  $X_0$ , was chosen. A similar thickness was allocated to the read-out and cooling systems, so the total amount of material per station has been engineered not to exceed 0.5% $X_0$ . Finally, the GTK must accommodate a high and non-uniform beam rate (0.75 MHz total, 1.3 MHz/mm<sup>2</sup> near the center) and survive a high radiation environment. No existing design meets all these requirements, and the resulting product, available for other applications, such as medicine, is a novel combined effort of numerous academic, research, and commercial institutions.

Charged particle tracking downstream of the decay volume will be done with Straw Trackers, which will be stationed in vacuum. With no beam windows or surrounding gas, the material budget is extremely small:  $\approx 0.1\%$   $X_0$  per layer. Each straw can maintain a 0.5 MHz rate with high efficiency. Four straw stations,

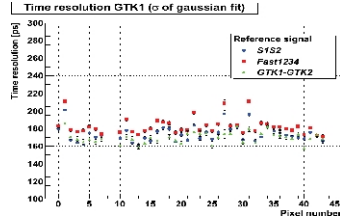


Figure 2: Time resolution for a GTK proto-type module in a test beam.

each with views in four coordinates ( $x$ ,  $y$ ,  $u$ ,  $v$ ), are positioned two each side of a spectrometer magnet. Each view has a position resolution of about  $130 \mu\text{m}$ . The angular resolution is expected to be  $10 \mu\text{rad}$  for 10-GeV pions and  $20 \mu\text{rad}$  for 60-GeV pions. The relative momentum resolution should be about 0.33%, and the extrapolated vertex resolution (closest distance of approach) should be about 1 mm. The stringing of the first straw module is complete [See Figure 3].

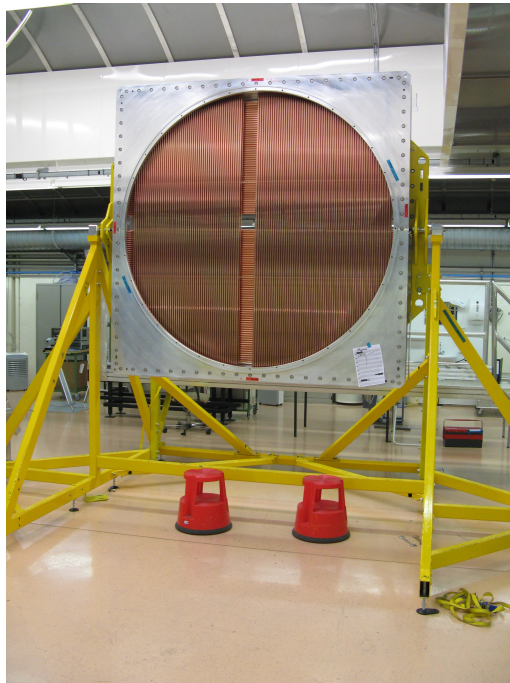


Figure 3: The first of sixteen straw modules has been strung.

Kinematic rejection allows differentiation of the signal from about 92% of the total  $K^+$  width. The discriminating kinematic variable is missing mass squared:

$$m_{\text{miss}}^2 = (\mathbf{P}_K - \mathbf{P}_\pi)^2 \quad (1)$$

In terms of this variable, two signal regions can be identified, between the  $K^+ \rightarrow \mu^+ \nu_\mu$  and  $K^+ \rightarrow \pi^+ \pi^+ \pi^-$  spectra, and separated by the  $K^+ \rightarrow \pi^+ \pi^0$  peak [see Figure 4]. The first region spans from about 0 to 0.01  $(\text{GeV}/c^2)^2$ , and the second region spans from about 0.025  $(\text{GeV}/c^2)^2$  to about 0.068  $(\text{GeV}/c^2)^2$ . The

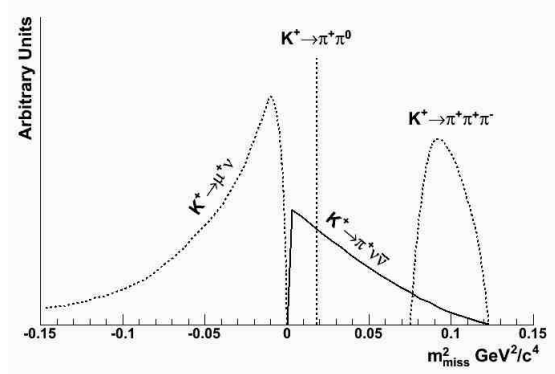


Figure 4: Kinematically constrained background.

remaining 8% or so of the width is not so constrained [see Figure 5].

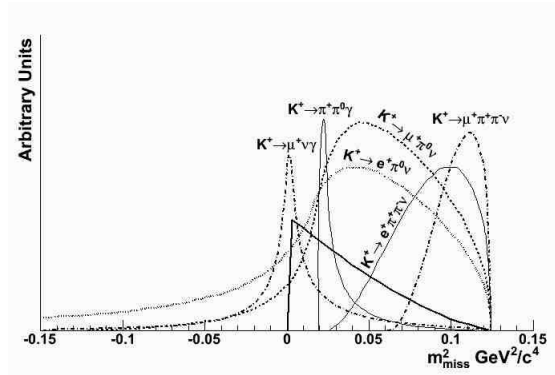


Figure 5: Kinematically unconstrained background.

The efficiency of this kinematic selection obviously depends both on the missing mass squared resolution and on the association of the parent  $K^+$  with its daughter  $\pi^+$ . The missing mass squared resolution has been estimated to be roughly  $0.001 (\text{GeV}/c^2)^2$  with a realistic GEANT 4 Monte Carlo simulation of the new tracking system [see Figure 6]. This allows a 14.4% geometrical acceptance (3.5% from the first region and 10.9% from the second), with two-body rejection power of  $10^{-4}$  for  $K^+ \rightarrow \pi^+ \pi^0$  and  $10^{-5}$  for  $K^+ \rightarrow \mu^+ \nu_\mu$ . About half the losses are due to restrictions on the pion momentum, due to the RICH detector operating efficiency and muon and photon rejection. The signal acceptance will of course be somewhat lower than 14.4% due to losses from such experimental exigencies as dead time and channel inefficiencies. Additional

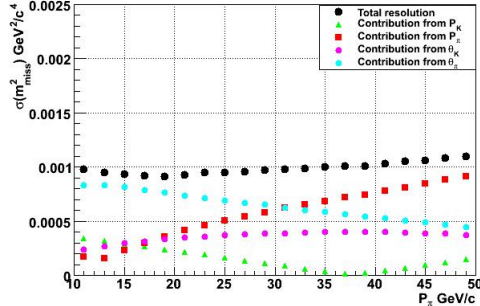


Figure 6: Missing mass squared resolution as a function of pion momentum.

signal efficiency loss will result from non-Gaussian tails in the missing mass squared distribution and from  $K - \pi$  mismatching.

To minimize the latter effect, which arises from the high-rate environment of the experiment, a differential Cerenkov counter will be employed to identify kaons, distinguishing them from pions and protons which might interact with the GTK or decay volume residual gas. The CEDAR detector will see a 50 MHz rate, while the GTK will experience an 800 MHz rate. Kaons will decay in the fiducial region at a rate of about 4.5 MHz, but the rate in the reconstruction detectors will be in the 7-10 MHz range, enhanced by a muon halo from upstream particle interactions and pion decay-in-flight. The demands on parent-daughter matching are compounded by the finite width and divergence of the charged particle beam. Design parameters call for  $\sigma(t) \approx 100$  ps for both  $K^+$  and  $\pi^+$  tracks.

The NA62 detector will include both photon and muon veto capabilities. Photon vetoing will enhance the detector's  $K^+ \rightarrow \pi^+\pi^0$  rejection power by identifying  $\pi^0$ s. With the charged pion momentum requirement  $p_{\pi^+} < 35$  GeV/c,  $p_{\pi^0} > 40$  GeV/c, and the daughter photons of the latter will consequently have energies in excess of 1 GeV. For 10 GeV photons, the liquid krypton calorimeter (LKr) (coverage from 1-8.5 mrad) has an inefficiency of  $10^{-5}$ .

Including large- (8.5-50 mrad) and small-angle photon veto detectors ( $< 1$  mrad) will increase the rejection factor for  $\pi^0$ s from  $K^+ \rightarrow \pi^+\pi^0$  to about  $10^{-8}$ . Six of twelve large-angle photon veto detectors have already been constructed at Frascati and delivered to CERN.

Muon vetoing will enhance the rejection power beyond kinematics of  $K^+ \rightarrow \mu^+\nu_\mu$ . A combination of detectors, including the liquid krypton calorimeter and the muon detector system, which can also serve as a hadron calorimeter, can separate minimum ionizing particles from electromagnetic and hadronic showers. The rejection factor for muons from  $K^+ \rightarrow \mu^+\nu_\mu$  is expected to be around  $10^{-5}$ .

All this, however, remains inadequate to suppress sufficiently the  $K^+ \rightarrow \mu^+\nu_\mu$  background, and even less so that from  $K^+ \rightarrow \mu^+\nu_\mu\gamma$ , which is unconstrained kinematically. Particle identification, with the liquid krypton calorimeter and RICH detector, can add another factor of  $10^{-2}$  to the rejection power, by distinguishing between pions and muons in the momentum range between 15 GeV/c and 35 GeV/c.

The RICH detector is expected to have excellent timing ( $\sigma_t \approx 100$  ps, offline), and as such, may be used in the lowest-level, hardware trigger. Primitive reconstruction algorithms, perhaps carried out with the aid of Graphical Processing Units, may allow for pion identification in the first software trigger.

Excellent timing and position resolution and particle identification within a hermetic detector can, with a high-flux kaon beam, lead to the background suppression and signal efficiency required to make a measurement of the  $K^+ \rightarrow \pi^+ \nu \bar{\nu}$  branching ratio of sensitivity that begins to challenge theoretical predictions. Table 1 summarizes the components of this sensitivity.

Table 1: Sensitivity and backgrounds.

Decay Channel	Events
<b>Signal:</b> $K^+ \rightarrow \pi^+ \nu \bar{\nu}$ [flux = $4.8 \times 10^{12}$ decays/year]	<b>55 events/year</b>
$K^+ \rightarrow \pi^+ \pi^0$ [ $\eta_{\pi^0} = 2 \times 10^{-8}$ ( $3.5 \times 10^{-8}$ )]	4.3% (7.5%)
$K^+ \rightarrow \mu^+ \nu_\mu$	2.2%
$K^+ \rightarrow e^+ \pi^+ \pi^- \nu_e$	$\leq 3\%$
Other 3 charged-track events	$\leq 1.5\%$
$K^+ \rightarrow \pi^+ \pi^0 \gamma$	$\sim 2\%$
$K^+ \rightarrow \mu^+ \nu_\mu \gamma$	$\sim 0.7\%$
$K^+ \rightarrow e^+ (\mu^+) \pi^0 \nu$ , others	negligible
<b>Expected Background/Signal Fraction</b>	$\leq$ <b>13.5% (17%)</b>

A test run of the experiment, with a subset of the final detector will take place in Autumn 2012. The primary focus of the run is the hardware trigger system, particularly its integration with detector subsystems and its potential for reducing raw rates by a factor of ten. Given CERN's current accelerator operation plan, first physics for NA62 is expected in 2014.